Maxillofacial bone regeneration with osteogenic matrix cell sheets: An experimental study in rats

Yoshihiro Ueyama[a], Takahiro Yagyuu[a,*], Masahiko Maeda[a], Mitsuhiko Imada[a], Manabu Akahane[b], Kenji Kawate[c], Yasuhito Tanaka[d], Tadaaki Kirita[a]

[a] Department of Oral and Maxillofacial Surgery, Nara Medical University, 840 Shijo-cho, Kashihara, Nara 634-8521, Japan
[b] Department of Public Health, Health Management and Policy, Nara Medical University, 840 Shijo-cho, Kashihara, Nara 634-8521, Japan
[c] Department of Artificial Joint and Regenerative Medicine for Bone and Cartilage, Nara Medical University, 840 Shijo-cho, Kashihara, Nara 634-8521, Japan
[d] Department of Orthopedic Surgery, Nara Medical University, 840 Shijo-cho, Kashihara, Nara 634-8521, Japan

ARTICLE INFO

ABSTRACT

Objective: Regeneration of maxillofacial bone defects, characterized by relatively small but complicated shapes, poses a significant clinical challenge. Osteogenic matrix cell sheets (OMCSs) have osteogenic ability and good shaping properties and may be ideal graft materials. Here, we assessed whether implantation of OMCSs could be used to repair maxillofacial bone defects.
Design: We adopted a rat mandibular symphysis model. The rat mandible is formed by a paired bone and the central portion consisting of fibrous tissue. There is no bone tissue at the site; accordingly, this site was interpreted as a physiological bone gap and was used for evaluation. Rat bone marrow cells were cultured in medium containing dexamethasone and ascorbic acid phosphate to create OMCSs. The OMCSs were implanted into the rat mandibular symphysis without a scaffold. Microcomputed tomography and histological analyses were conducted after 2, 4, and 8 weeks.
Results: Two weeks after implantation, microcomputed tomography images and histological sections showed some sparse granular calcification tissue within the bone gap at the mandibular symphysis. At 4 weeks, the calcification tissue spread, and the gap of the mandibles were continued. At 8 weeks, this continuous new bone tissue was matured. The experimental group showed abundant new bone tissue in the group with OMCS implantation, but not in the group with sham implantation.
Conclusions: Our present results indicated that use of OMCSs may be an optimal approach towards achieving maxillofacial regeneration.

© 2016 Elsevier Ltd. All rights reserved.

1. Introduction

Maxillary alveolar cleft, facial trauma, bone resection due to cancer, periodontal disease, and bone atrophy after tooth extraction may result in non-healing maxillofacial bone defects. Autologous bone grafts are considered the gold standard for repairing such bone defects (Behnia et al., 2009; Liu, Tan, Luo, Hu, & Yue, 2014; Xie et al., 2007; Yoshioka et al., 2012). However, donor site morbidity is an important consideration. Maxillofacial bone defects are often smaller than those commonly encountered in orthopedic surgery, but have more complicated morphology (d'Aquino et al., 2009). Thus, the ability of the graft material to assume a complex shape is essential for maxillofacial bone regeneration.

Recently, researchers have been working to develop cell-based bone repair methods as a substitute for autologous bone grafts (Kawate et al., 2006; Morishita et al., 2006). We previously developed a cell transplantation method based on cell sheet technology with bone marrow-derived stromal cells (BMSCs), which were cultured in the presence of dexamethasone (Dex) and ascorbic acid phosphate (Akahane et al., 2008). These cells were lifted as cell sheets, termed osteogenic matrix cell sheets (OMCSs),

with no special materials, such as thermosensitive polymers. OMCSs can be transplanted without a scaffold, resulting in bone formation (Inagaki et al., 2013; Nakamura et al., 2010). OMCSs are sufficiently malleable that they may represent optimal graft materials for maxillofacial bone regeneration. However, transplantation of OMCSs at the site of maxillofacial bone defects has not yet been attempted.

Recently, the rat mandibular symphysis, i.e., the central portion of the rat mandible, which consists of fibrous connective tissue and thus can be interpreted as a physiological bone gap, has been used to assess bone graft materials, particularly for the purpose of maxillofacial bone regeneration (Yagyuu, Kirita, Hattori, Tadokoro, & Ohgushi, 2015). Therefore, in this study, we adopted a rat mandibular symphysis model and examined whether implantation of OMCSs could fill the gap with new bone tissue, leading to bone union.

2. Materials and methods

2.1. Animals

All animal studies were approved by the animal care and use committee of Nara Medical University before beginning the experiments. Fischer 344 (F344) rats were purchased from Japan SLC, Inc. (Hamamatsu, Japan). Seven-week-old male rats were used as donors for marrow cell preparation, and 15-week-old rats were used as recipients.

2.2. Cell culture and cell sheet preparation

OMCSs were used in this study and were prepared as previously reported (Akahane et al., 2008; Inagaki et al., 2013; Nakamura et al., 2010). In brief, rat bone marrow plugs were flushed out and resuspended in basic culture medium, i.e., minimum essential medium (Nacalai Tesque Inc., Kyoto, Japan) containing 15% fetal bovine serum (Gibco, Invitrogen, CA, USA) and 1% antibiotics (100 U/mL penicillin and 100 μg/mL streptomycin; Nacalai Tesque Inc.). Cells were cultured in T-75 flasks in a humidified atmosphere of 95% air with 5% CO_2 at 37 °C. After reaching confluence, the primary cultured cells were harvested using trypsin/ethylenediaminetetraacetic acid (Gibco, Invitrogen). To generate the OMCSs, the harvested cells were seeded at a cell density of 1×10^4 cells/cm^2 in 6-cm culture dishes with basic culture medium, 10 nM Dex (Sigma-Aldrich, MO, USA), and 0.28 mM ascorbic acid phosphate (Wako Pure Chemical Industrials, Kyoto, Japan) and then subcultured. After reaching confluence, the cells were rinsed twice with phosphate-buffered saline (Gibco, Invitrogen) and then formed into a sheet using a scraper (Fig. 1A).

2.3. In vitro evaluation of OMCSs

Samples of the OMCSs were fixed in 10% formaldehyde neutral buffer solution for 1 week and embedded in paraffin. Each specimen was cut into 5-μm sections, and the sections were stained with hematoxylin and eosin (H&E). Immunohistochemical staining for type I collagen, osteopontin (OPN), and osteocalcin (OCN) was performed on 5-μm sections mounted on glass slides. To enhance antigen retrieval, all sections were treated with 3% hydrogen peroxidase for 10 min to block endogenous peroxidase activity and subsequently blocked for 10 min at 37 °C with 1% bovine serum albumin, followed by overnight incubation at 4 °C with specific primary antibodies, including anti-type I collagen (LB1102; LSL, Inc., Japan; 1:500 dilution), anti-OPN (01-0091; ARP, Inc., USA; 1:100 dilution), and anti-OCN (M186; TaKaRa Bio, Inc., Japan; 1:100 dilution).

The slides were then rinsed and incubated for 30 min at 37 °C with biotinylated secondary antibodies. The slides were then washed with Tris-buffered saline, and peroxidase-streptavidin was added for 30 min at 37 °C. Finally, the slides were rinsed well with Tris-buffered saline and developed with 3,3′-diaminobenzidine.

2.4. Implantation protocol

Prior to implantation, we folded the OMCSs into a lump, 2-mm in diameter (Fig. 1B). Shortly thereafter, we implanted the OMCSs into the mandibular symphysis of recipient 15-week-old syngeneic rats, as previously reported (Yagyuu et al., 2015). Briefly, we anesthetized each rat with pentobarbital and shaved the incision site (Fig. 1C). An incision was created in the skin at the inferior margin of the mandible. After exposure of the periosteum of the left and right mandibles, the periosteum was incised and separated. The fibrous tissue between the left and right mandibles was then curetted, creating space for the implant (Fig. 1D). Finally, we implanted a lump of OMCSs into the space (Fig. 1E) and closed the periosteum and skin layers separately. We performed this procedure in 30 rats (experimental group); an additional 10 rats underwent surgery without implantation (control group). Ten animals were sacrificed at each time point (2, 4, and 8 weeks postoperatively) in the experimental group, and 10 animals were sacrificed at 8 weeks postoperatively in the control group. The mandibles were compared using micro-computed tomography (micro-CT) and histological analyses to evaluate the ability of OMCSs to fill the bone at the mandibular symphysis.

2.5. Micro-CT analyses

The harvested rat mandibles were analyzed using a micro-CT (Toscaner–32300 μ-FPD; Toshiba IT and Control Systems Corp., Tokyo, Japan). Each mandible was scanned at intervals of 10 μm at 70 kV and 200 μA. Three-dimensional images were constructed using VG Studio software (Volume Graphics, Heidelberg, Germany). The images were evaluated semiquantitatively using a radiological union scale (Table 1) (Yagyuu et al., 2015). Furthermore, we evaluated the new bone volume. We measured an area of calcification in the mandibular symphysis as a high-density area, defined as a density equal to or greater than 220 CT units, within the region of interest (ROI). To set the ROI, we first established the axial plane perpendicular to the occlusal plane of the molar teeth and on the distal side, 2 mm farther than the plane including the lowest point of the chin, i.e., the menton. In this plane (transverse plane), we defined an ROI as a square area 1.0 mm in height and 1.0 mm in width positioned in the mandibular symphysis. The calcification area (mm^2) was measured using ImageJ software (v. 1.49; NIH, USA).

2.6. Histological analysis

After micro-CT analysis, mandibles from each group of rats were fixed in 10% formaldehyde neutral buffer solution, decalcified (K-CX; Falma Inc., Tokyo, Japan), embedded in paraffin, and stained with H&E and toluidine blue solution. The histological sections were evaluated using a histological union scale (Table 1) (Yagyuu et al., 2015). Next, we performed histomorphometric analysis. We established an ROI as a square area 1.0 mm in height and 1.0 mm in width positioned between the left and right mandibles in the histological slide of the transverse plane, and the new bone formation area (mm^2) was measured using ImageJ software.
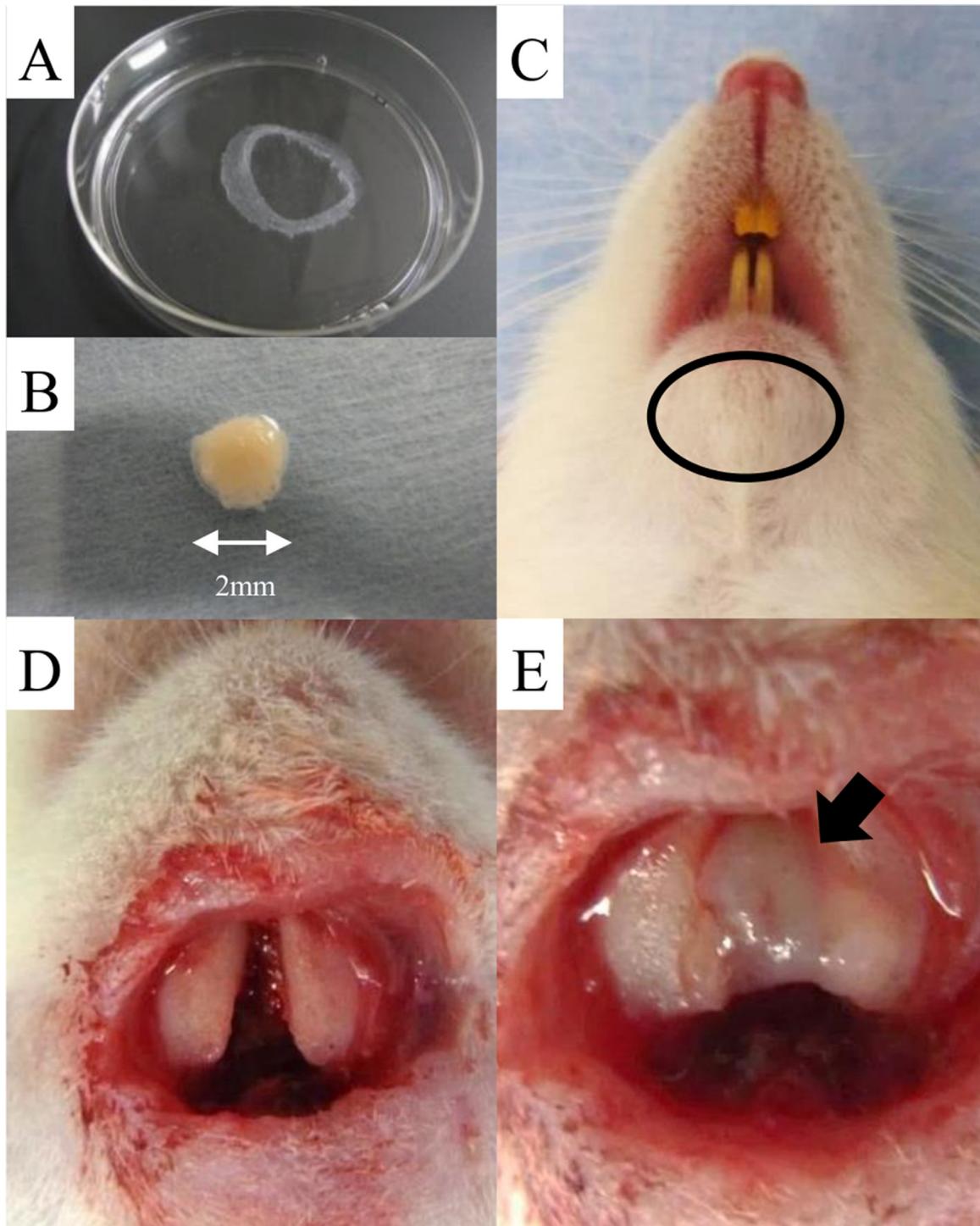
Fig. 1. Implantation technique. (A) OMCSs were easily detached from the culture dish using a scraper. (B) OMCSs were folded to form a lump, 2-mm in diameter. (C) An incision of about 10-mm was made in the skin over the inferior margin of the mandible (circle). (D) The fibrous tissue occupying the mandibular symphysis was curetted to create space for the implant. (E) OMCSs were implanted into the mandibular symphysis (arrow).

2.7. Statistical analysis

Radiological and histological union scale scores for the samples were evaluated using Mann-Whitney *U*-tests. The statistical significance of differences in the calcification area determined by micro-CT analysis and new bone formation area determined by histomorphometric analysis were determined using Student's *t*-tests. Differences with *p* values of less than 0.05 were considered significant for both tests.

3. Results

3.1. In vitro evaluation of OMCSs

H&E-stained sections revealed that the OMCSs comprised several cell layers laminated along the sheet with abundant extracellular matrices (Fig. 2A). Immunohistochemical studies revealed that type I collagen was strongly expressed in the

Table 1
Radiological and histological union scales.

Score	Description
Radiological union scale	
0	No noticeable new bone formation
1	Cortical bone thickening along the margins of the mandibular symphysis
2	Bone union with apparent cracks/fissures
3	Bone union with or without trace of cracks/fissures
Histological union scale	
0	Fibrous union with trace of new cartilage/bone formation
1	Fibrous union with some new cartilage/bone areas
2	Bone union with cartilaginous areas
3	Complete bone union without cartilaginous areas
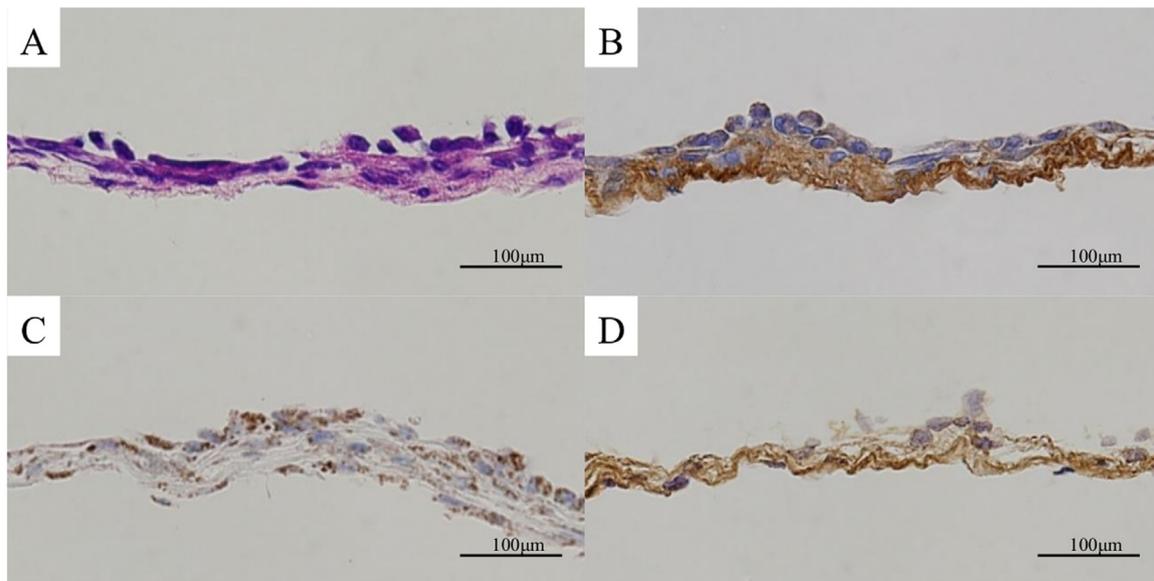
Fig. 2. *in vitro* evaluation of OMCSs. (A) H&E-stained section of OMCSs showing an abundance of cells and extracellular matrices. (B) Strongly positive staining for type I collagen was observed in the extracellular matrix. (C) Positive staining for osteopontin was observed in the cytoplasm of the cultured cells. (D) Positive staining for osteocalcin was observed in the extracellular matrix.

matrices secreted by the cultured BMSCs (Fig. 2B). Furthermore, OPN and OCN were expressed in the cultured cells (Fig. 2C and D).

3.2. Comparison of micro-CT images

Two weeks after implantation of OMCSs, the micro-CT scans exhibited sparse areas of calcification within the bone gap at the mandibular symphysis (Fig. 3A). At 4 weeks, calcification had spread throughout the gap of the symphysis, and a porous calcified mass had formed, creating continuous bone tissue between the left and right sides of the mandibles (Fig. 3B). In 5 of 10 rats, the shape of the newly formed calcified mass resembled an OMCS lump implanted in the bone gap (Fig. 3B, upper images). At 8 weeks, the surface of the newly formed bone was smoother and more harmonized with the parent bone (Fig. 3C). In the control group 8 weeks after sham implantation, all rats showed irregular cortical bone thickening and resorption along the borders of the mandibles facing the mandibular symphysis; no rats exhibited bone union (Fig. 3D).

Next, we compared each group by semiquantitative evaluation of bone formation. Two weeks after implantation, eight rats in the experimental group received a radiological union score of 1, and the remaining two rats received a score of 0. Four weeks after implantation, nine rats in the experimental group received a radiological union score of 2, and the remaining rat received a score of 1. Eight weeks after implantation, six rats in the experimental group received a radiological union score of 3, and the remaining four rats received a score of 2. On the other hand, all 10 rats in the control group at 8 weeks after sham implantation received a score of 0. Thus, rats in the experimental group at 2, 4, and 8 weeks received significantly higher radiological union scores than did rats in the control group at 8 weeks ($p = 0.002$, $p = 0.0002$, and $p = 0.0002$, respectively, versus the control group; Table 2).

In addition, we evaluated the volume of new bone formation within the ROI in the mandibular symphysis. The mean values of the new bone formation area were $0.29 \pm 0.18 \, \text{mm}^2$ at 2 weeks, $0.70 \pm 0.12 \, \text{mm}^2$ at 4 weeks, and $0.93 \pm 0.06 \, \text{mm}^2$ at 8 weeks after implantation of OMCSs, compared with $0.08 \pm 0.05 \, \text{mm}^2$ in the control group at 8 weeks after sham implantation. There were significant differences between time points in the experimental group ($p = 7.3\text{E-}6$ for 2 versus 4 weeks, $p = 5.4\text{E-}5$ for 4 versus 8 weeks; Fig. 4A)

3.3. Comparison of histological analyses

Histological analyses revealed that remnants of immature cellular osteoids occupied the mandibular symphysis 2 weeks after implantation of OMCSs (Fig. 5A and B). Although the CT images
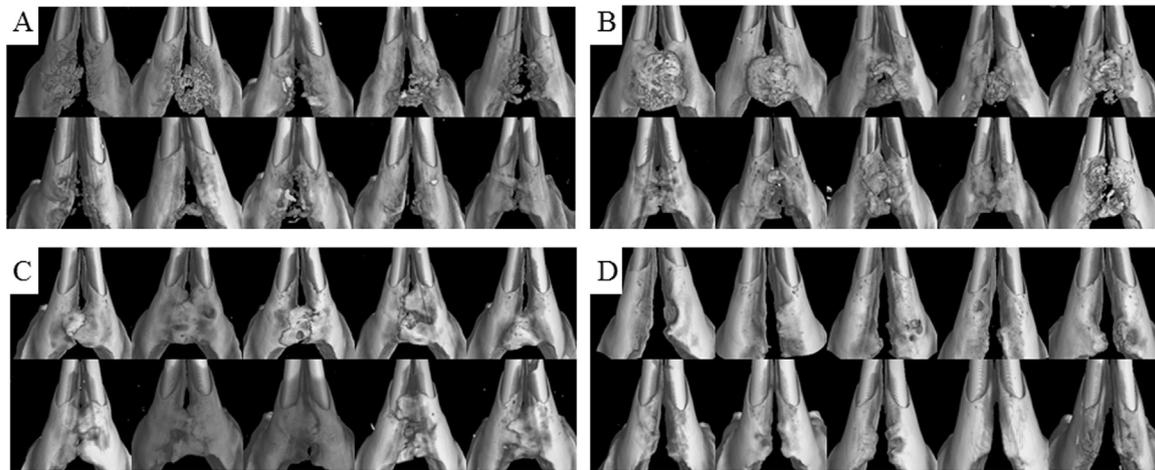
Fig. 3. Micro-CT analysis after surgery. (A) New bone formation was observed at 2 weeks in the experimental group. The images showed sparse areas of calcification in the mandibular symphysis. (B) Micro-CT scans 4 weeks after implantation showed bone continuation between the left and right sides of the mandibles with a porous calcified mass. (C) Micro-CT scans 8 weeks after implantation showed abundant bone formation occupying the mandibular symphysis. Six rats in this group showed complete bone union. (D) The control group had little bone formation in the mandibular symphysis.

Table 2
Results of radiological and histological union scales.

Score	Radiological scale				Histologiacal scale			
	Control	2 weeks	4 weeks	8 weeks	Control	2 weeks	4 weeks	8 weeks
0	10	2	0	0	10	0	0	0
1	0	8	1	0	0	5	0	0
2	0	0	9	4	0	5	1	0
3	0	0	0	6	0	0	9	10
		$p = 0.002^*$	$p = 0.0002^*$	$p = 0.0002^*$		$p = 0.0002^*$	$p = 0.0002^*$	$p = 0.0002^*$

* vs Control.
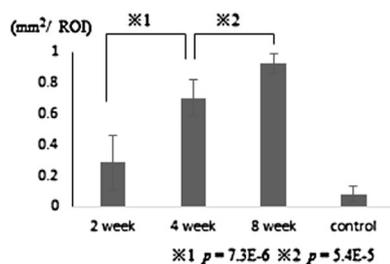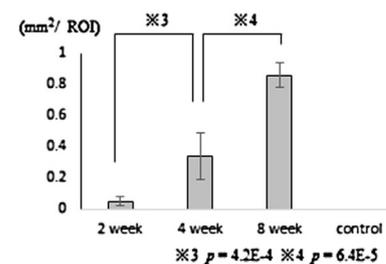
Fig. 4. The volume of new bone formation, as determined by micro-CT data and histomorphometric analysis. (A) Trend in the mean volume of new bone formation in the mandibular symphysis at 2, 4, and 8 weeks after implantation of OMCSs, showing an increase in volume over time. The increase was only slight in the control group at 8 weeks after sham implantation. (B) The newly formed bone area in the mandibular symphysis increased with time in the histomorphometric analysis. The error bar represents one standard deviation.

showed sparse areas of calcification within the bone gap, histological images demonstrated cartilaginous bone union between the left and right sides of the mandibles. Four weeks after implantation of OMCSs, anastomosing woven bone trabeculae had formed, rimmed with cuboid osteoblasts (Fig. 5C and D). Bone continuation between the left and right sides of the mandibles was observed. Eight weeks after implantation of OMCSs, calcification had advanced further, and the anastomosing, thick bony trabeculae were firmly attached to the adjacent parent bone (Fig. 5E–G). Cracks and fissures were observed in the newly formed bone by micro-CT analysis (Fig. 5H, arrow; corresponding to a score of 2 on the radiological union scale) and were caused by

cartilage tissue formation, as evidenced by H&E and toluidine blue staining (Fig. 5E and G). Additionally, this staining corresponded to an area of cracks and fissures in the new bone on the CT images. On the other hand, bone continuation was not observed in any mandibles in the control group (Fig. 5I–L), and fibrous tissue filled the mandibular bone gap. Similar to the results of semiquantitative evaluation of micro-CT analyses, the experimental group at 2, 4, and 8 weeks received significantly higher radiological union scores than did the control group at 8 weeks ($p = 0.0002$, $p = 0.0002$, and $p = 0.0002$, respectively, versus the control group; Table 2).

In the histomorphometric analysis, the mean new bone formation areas were 0.05 ± 0.12 mm^2 at 2 weeks, 0.34 ± 0.14 mm^2 at 4
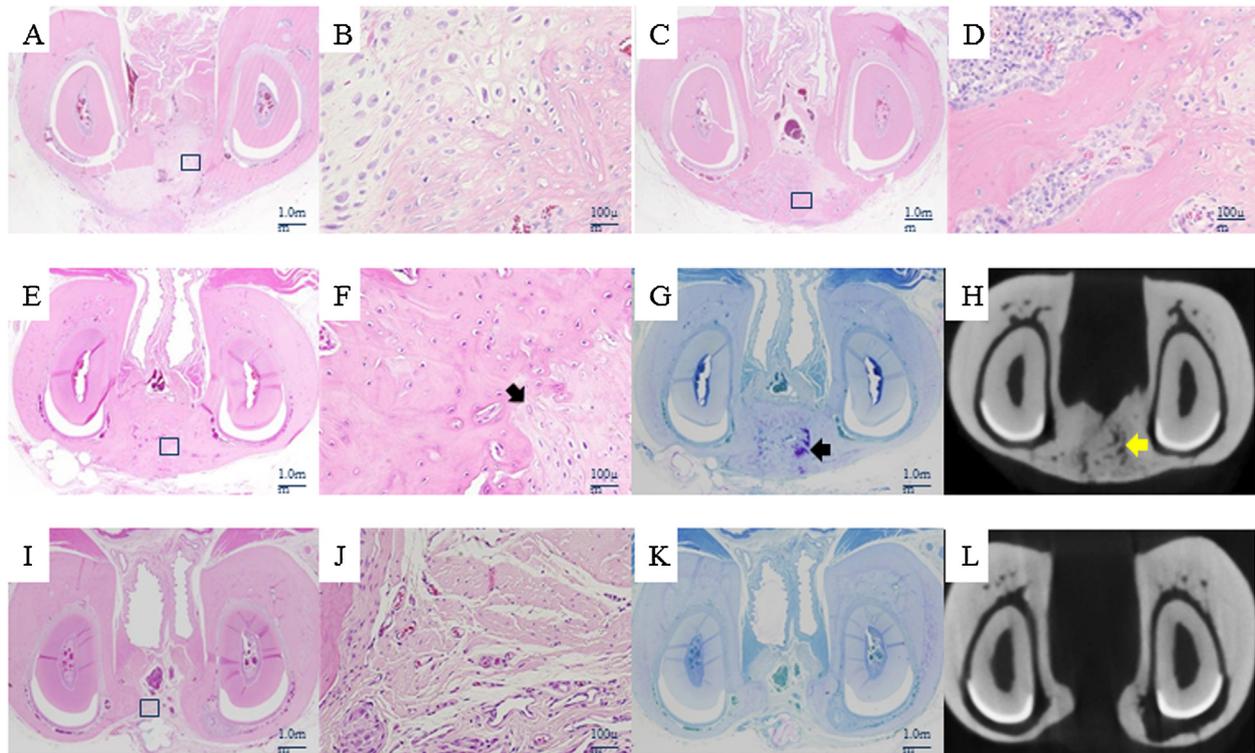
Fig. 5. Representative histological and radiological sections of the transverse view after surgery. (A) Representative H&E-stained sections 2 weeks after implantation, showing abundant fibrocartilage tissue in the mandibular symphysis, which formed a cartilaginous continuation between the left and right sides of the mandibles. (B) Magnified view of (A) showing immature cellular osteoids. (C) H&E-stained sections 4 weeks after implantation showing bone continuation between the left and right sides of the mandibles with woven bone trabeculae. (D) Magnified view of (C) showing newly formed bone rimmed with many cuboid osteoblasts. (E) H&E staining in the experimental group at 8 weeks after implantation, showing formed bone continuation between the left and right sides of the mandibles. (F) Magnified view of the rectangular area in (E) showing thick bony trabeculae. The black arrow indicates cartilage tissue. (G) Toluidine blue staining in the experimental group, showing cartilage tissue (black arrow) in the newly formed bone. (H) A cross-sectional image approximately corresponding to the histological sections in (E) and (G) reconstructed from the micro-CT image. Cracks and fissures (yellow arrow) in the newly formed bone, appearing as bone defects, were determined to be cartilage tissue by H&E staining [black arrow in (F)] and toluidine blue staining [black arrow in (G)]. (I) H&E staining in the control group showed no bone continuation between the left and right sides of the mandibles. (J) Magnified view of the rectangular area in (I) showing fibrous tissue with small vessels and little infiltration of inflammatory cells. (K) Toluidine blue staining of the control group did not detect cartilage tissue in the mandibular symphysis. (L) Cross-sectional image approximately corresponding to the histological sections in (I) and (K), reconstructed from the micro-CT image. Unlike in the experimental group, bone continuation was not observed.

weeks, and $0.86 \pm 0.10 \, \text{mm}^2$ at 8 weeks after implantation. In contrast, in the control group, the area was minimal at 8 weeks after sham implantation. In the experimental group, the new bone formation area increased over time (Fig. 4B).

4. Discussion

Cell sheet technology is a tissue engineering approach that does not require scaffolds (Matsuda, Shimizu, Yamato, & Okano, 2007; Matsuura, Utoh, Nagase, & Okano, 2014). Confluent cultures of cells can be harvested as a cell sheet without protease treatment. Avoiding protease treatment preserves complete cell–cell junctions, cell surface proteins, and the extracellular matrix in the cell sheet. Cell sheets are also soft, malleable, and easily molded. Cell sheet technology has been applied clinically in ocular surface disease (Burillon et al., 2012), heart disease (Sawa et al., 2012), and esophageal mucosa after surgery (Kobayashi et al., 2014). Cell sheet implantation has also been performed clinically for bone repair associated with artificial bones (Iwata et al., 2015; Kaushick, Jayakumar, Padmalatha, & Varghese, 2011; Okuda et al., 2009; Yamamiya et al., 2008). However, it is unclear whether cell sheets can be used to repair natural bone defects without scaffolds (Ma et al., 2011). In this study, we sought to examine the therapeutic potential of OMCSs used alone for bone defects.

OMCSs are prepared from BMSCs originating from the mesoderm. Although the efficacy of OMCSs for regeneration of long bones, whose origins are the same as that of BMSCs, has previously been reported (Nakamura et al., 2010), it is unclear whether OMCSs can be applied for repair of maxillofacial bones. The developmental cascade and origins of long bones are different from those of maxillofacial bones. Long bones are of mesodermal origin and are generated by endochondral ossification, whereas maxillofacial bones are of neuroectodermal origin and are generated by membranous ossification. Therefore, in this study, we adopted a rat mandibular symphysis model and investigated whether OMCSs could repair maxillofacial bone.

Our current model made use of the mandibular symphysis (Yagyuu et al., 2015). The rat lower jaw does not have continuous bone. Instead, fibrous tissue is present between the left and right sides of the mandibles in the mandibular symphysis. In other words, the symphysis can be considered a natural bone defect that never heals. Thus, we simply curetted the interposed fibrous tissue and implanted the OMCSs. Micro-CT and histological analyses demonstrated bone continuation between the left and right sides of the mandibles 4 weeks after OMCS implantation, but not in sham implantation, even at 8 weeks. These data demonstrated the therapeutic potential of OMCSs alone for repairing bone defects. Moreover, OMCSs could be used in maxillofacial bones that originate from the neuroectoderm.

In this study, we used micro-CT for radiological analysis. Micro-CT is a useful and reliable method for evaluating bone healing. Alternatively, histomorphometry is considered the gold standard for evaluating bone healing as it facilitates in situ analysis of bone cells as well as their activities (Acar et al., 2015, 2016). Ezirganlı, Polat, Barış, Tatar, and Çelik (2013) reported that there was a correlation between micro-CT and histomorphometric analysis. In this study, according to the results of both micro-CT and histomorphometry, new bone formation in the mandibular symphysis increased over time; both analyses yielded similar results.

A time-series evaluation of the implanted OMCSs revealed that the OMCSs became bone tissue and that the morphology of the ossified OMCSs reflected local mechanical stress. That is, bone tissue formed from OMCSs could remodel itself in accordance with Wolff's law (Wolff, 1891).

Previously, we implanted cultured bone (rat BMSC-ceramic composites) into the present rat model; bone union between the left and right sides of the mandibles occurred following implantation of the cultured bone (Yagyuu et al., 2015). We also performed a clinical trial in which we implanted the cultured bone into maxillofacial bone defects (approved by the Ministry of Health, Labour and Welfare of Japan, May 28, 2010). To manufacture the cultured bone, we first expanded the number of BMSCs collected from the iliac crest of each patient and then cultured the cells with β-tricalcium phosphate (TCP) granules in osteoinductive medium for generation of a BMSC–β-TCP composite as cultured bone. The manufacturing process for the cultured bone required about 6 weeks. A process this long not only increases the risk of contamination or infection, but also significantly increases costs. In this regard, OMCSs have advantages over cultured bone and can be created in a much shorter time period. To create OMCSs, BMSCs are simply expanded in osteoinductive medium, and it is not necessary to culture cells on artificial bone. Therefore, we estimate that the process could be shortened to about 4 weeks.

Additionally, using OMCSs, the number of cells necessary for implantation may be less than that required to manufacture cultured bone, although a direct comparison was not performed. In our previous study with cultured bone, 1×10^7 implanted cells were needed for bone union in the present rat model (Yagyuu et al., 2015), whereas only 2×10^5 cells were required to achieve the same results in the present study (data not shown). These results are likely due to the properties of OMCSs, which are harvested with many intact bone matrix components and cell–cell contacts (Akahane et al., 2008; Nakamura et al., 2010). In vitro evaluation of the OMCSs also revealed that the cells were surrounded by abundant protein matrices containing type I collagen, OPN, and OCN, which may promote osteogenesis.

Although our data demonstrated that OMCSs may have useful and promising applications in bone regeneration, OMCSs have poor mechanical properties. Indeed, previous studies have recommended the use of artificial bone along with OMCSs for this reason (Nakamura et al., 2010). However, we believe that OMCSs can be used for bone defects with low mechanical stress. Maxillofacial bone defects occur in low stress-bearing bones compared with those in orthopedic surgery. Moreover, maxillofacial bone defects are generally smaller than orthopedic defects, but can have more complicated shapes. Therefore, OMCSs, which have poor mechanical properties but good shaping properties, may be an optimal graft material for regeneration of maxillofacial bone defects. Further studies are needed to determine whether OMCSs have applications in the clinical treatment of maxillofacial bone defects.

In conclusion, we confirmed the efficacy of implanting OMCSs alone using a rat mandibular symphysis model. OMCSs may be an optimal graft material for regeneration of maxillofacial bone defects.

Funding

Competing interests

None of the authors have any conflicts of interest regarding this research.

Ethical approval

This study was approved by the animal care and use committee of Nara Medical University (protocol No. 10483).

References

Acar, A. H., Yolcu, Gül, M., Keleş, A., Erdem, N. F., & Altundag Kahraman, S. (2015). Micro-computed tomography and histomorphometric analysis of the effects of platelet-rich fibrin on bone regeneration in the rabbit calvarium. Archives of Oral Biology, 60, 606–614.

Acar, A. H., Yolcu, Altındiş, S., Gül, M., Alan, H., & Malkoç, S. (2016). Bone regeneration by low-level laser therapy and low-intensity pulsed ultrasound therapy in the rabbit calvarium. Archives of Oral Biology, 61, 60–65.

Akahane, M., Nakamura, A., Ohgushi, H., Shigematsu, H., Dohi, Y., & Takakura, Y. (2008). Osteogenic matrix sheet-cell transplantation using osteoblastic cell sheet resulted in bone formation without scaffold at an ectopic site-. Journal of Tissue Engineering and Regenerative Medicine, 2, 196–201.

Behnia, H., Khojasteh, A., Soleimani, M., Tehranchi, A., Khoshzaban, A., Keshel, S. H., et al. (2009) Secondary repair of alveolar clefts using human mesenchymal stem cells. 108, e1–e6.

Burillon, C., Huot, L., Justin, V., Nataf, S., Chapuis, F., Decullier, E., et al. (2012). Cultured autologous oral mucosal epithelial cell sheet (CAOMECS) transplantation for the treatment of corneal limbal epithelial stem cell deficiency. Investigative Ophthalmology and Visual Science, 13, 1325–1331.

d'Aquino, R., De Rosa, A., Lanza, V., Tirino, V., Laino, L., Graziano, A., et al. (2009). Human mandible bone defect repair by the grafting of dental pulp stem/progenitor cells and collagen sponge biocomplexes. European Cells & Materials, 12, 75–83.

Ezirganlı, S., Polat, S., Barış, E., Tatar, I., & Çelik, H. H. (2013). Comparative investigation of the effects of different materials used with a titanium barrier on new bone formation. Clinical Oral Implants Research, 24, 312–319.

Inagaki, Y., Uematsu, K., Akahane, M., Morita, Y., Ogawa, M., Ueha, T., et al. (2013). Odontgenic matrix cell sheet transplantation enhances early tendon graft to bone tunnel Healing in rabbits. BioMed Research International. http://dx.doi.org/10.1155/2013/842192,2013.

Iwata, T., Washio, K., Yoshida, T., Ishikawa, I., Ando, T., Yamato, M., et al. (2015). Cell sheet engineering and its application for periodontal regeneration. Journal of Tissue Engineering and Regenerative Medicine, 9, 43–356.

Kaushick, B. T., Javakumar, N. D., Padmalatha, O., & Varghese, S. (2011). Treatment of human periodontal intrabony defects with hydroxyapatite beta tricalcium phosphate bone graft alone and in combination with platelet rich plasma a randomized clinical trial. Indian Journal of Dental Research, 22, 505–510.

Kawate, K., Yajima, H., Ohgushi, H., Kotobuki, N., Sugimoto, K., Ohmura, T., et al. (2006). Tissue-engineered approach for the treatment of steroid-induced osteonecrosis of the femoral head: Transplantation of autologous mesenchymal stem cells cultures with beta-tricalcium phosphate ceramics and free vascularized fibula. Artificial Organs, 30, 960–962.

Kobayashi, S., Kanai, N., Ohki, T., Takagi, R., Yamaguchi, N., Isomoto, H., et al. (2014). Prevention of esophageal strictures after endoscopic submucosal dissection. World Journal of Gastroenterology, 7, 15098–15109.

Liu, C., Tan, X., Luo, J., Hu, M., & Yue, W. (2014). Reconstruction of beagle hemi-mandibular defects with allogenic mandibular scaffolds and autologous mesenchymal stem cells. PUBLIC LIBRARY OF SCIENCE, 25, e105733.

Ma, D., Yao, H., Tian, W., Chen, F., Liu, Y., Mao, T., et al. (2011). Enhancing bone formation by transplantation of a scaffold-free tissue engineered periosteum in a rabbit model. Clinical Oral Implants Research, 22, 1193–1199.

Matsuda, N., Shimizu, T., Yamato, M., & Okano, T. (2007). Tissue engineering based on cell sheet technology. Advanced Materials, 19, 3089–3099.

Matsuura, K., Utoh, R., Nagase, K., & Okano, T. (2014). Cell sheet approach for tissue engineering and regenerative medicine. Journal of Controlled Release. http://dx.doi.org/10.1016/j.jconrel.2014.05.024.

Morishita, T., Honoki, K., Ohgushi, H., Kotobuki, N., Matsushima, A., & Takakura, Y. (2006). Tissue engineering approach to the treatment of bone tumors: Three cases of cultured bone grafts derived from patients' mesenchymal stem cells. Artificial Organs, 30, 115–118.

Nakamura, A., Akahane, M., Shigematsu, H., Tadokoro, M., Morita, Y., Ohgushi, H., et al. (2010). Cell sheet transplantation of cultured mesenchymal stem cells enhances bone formation in a rat nonunion model. *Bone, 46,* 418–424.

Okuda, K., Yamamiya, K., Kawase, T., Mizuno, H., Ueda, M., & Yoshie, H. (2009). Treatment of human infrabony periodontal defects by grafting human cultured periosteum sheets combined with platelet-rich plasma and porous hydroxyapatite granules:case series. *Journal of the International Academy of Periodontology, 11,* 206–213.

Sawa, Y., Miyagawa, S., Sakaguchi, T., Fujita, T., Matsuyama, A., Saito, A., et al. (2012). Tissue engineered myoblast sheets improved cardiac function sufficiently to discontinue LVAS in a patient with DCM: Report of a case. *Surgery Today, 42,* 181–184.

Wolff, J. (1891). Ueber die Theorie des Knochenschwundes durch vermehrten Druck und der Knochenanbildung durch Druckentlastung. *Archivs Für Klin Chirurgie, 42,* 302–324.

Xie, C., Reynolds, D., Awad, H., Rubery, P. T., Pelled, G., Gazit, D., et al. (2007). Structural bone allograft combined with genetically engineered mesenchymal stem cells as a novel platform for bone tissue engineering. *Tissue Engineering, 13,* 435–445.

Yagyuu, T., Kirita, T., Hattori, K., Tadokoro, M., & Ohgushi, H. (2015). Unique and reliable rat model for the assessment of cell therapy: Bone union in the rat mandibular symphysis using bone marrow stromal cells. *Journal of Tissue Engineering and Regenerative Medicine, 9,* 276–285.

Yamamiya, K., Okuda, K., Kawase, T., Hata, K., Wolff, L. F., & Yoshie, H. (2008). Tissue-engineered cultured periosteum used with platelet rich plasma and hydroxyapatite in treating human osseous defects. *Journal of Periodontology, 79,* 811–818.

Yoshioka, M., Tanimoto, K., Tanne, Y., Sumi, K., Awada, T., Oki, N., et al. (2012). Bone regeneration in artificial jaw cleft by use of carbonated hydroxyapatite particles and mesenchymal stem cells derived from ilac bone. *International Journal of Dentistry.* http://dx.doi.org/10.1155/2012/352510.